A Static Pile Load Test on a Bored Pile Instrumented with Distributed Fibre Optic Sensors

Jakub Kania
cp test a/s and Aarhus University, Vejle / Aarhus, Denmark, jakub@cptest.dk / jgk@eng.au.dk

Kenny Kataoka Sørensen
Aarhus University, Aarhus, Denmark, kks@eng.au.dk

SUMMARY: This paper presents a case study of a static pile load test on an instrumented 630 mm diameter cased CFA pile installed in sand at a site located in Viborg, Denmark. The test was conducted to obtain the load-movement relationship, the distribution of strain and stresses along the pile and to compare the readings from conventional strain gauges and distributed fibre optic sensors for measuring internal pile strains. For this purpose, the pile was instrumented with vibrating wire sister bar strain gages in addition to fibre optic strain and temperature cables along the full length of the pile. The pile was loaded incrementally at the pile head in two loading cycles. It was found that the distributed fibre optic sensors gave strain measurement in good agreement with those obtained from conventional strain gauges and that they can provide detailed information of stress and strain distribution along the full length of a pile.

KEYWORDS: static pile load test, bored pile, field instrumentation, distributed fibre optic sensing

1 INTRODUCTION

One of the most reliable test to assess a bored pile capacity is a static pile load test. Unfortunately, during the test only the movement of a pile head subjected to a given load is measured. More comprehensive results can be obtained with dedicated pile instrumentation. Traditionally, bored concrete piles have been instrumented with simple telltales to achieve a measurement of pile deformation relative to the pile head (Dunnicliff, 1993) or in recent decades more commonly with spot measurement using vibrating wire (or electrical) embedded or sister bar strain gauges (Dunnicliff, 1993, Fellenius, 2002, Siegel and McGillivray, 2009). The typical gauge length of single point strain gauges range from around 50 mm to 250 mm. Recent developments in the field of distributed fibre optic sensors have shown the possibility of implementing low cost distributed fibre optic sensors in civil engineering for obtaining high resolution strain measurements in structures. While the majority of reported studies are based on measurements from distributed fiber optic sensors taken using interrogators based on Brillouin scattering (Kechavarzi et al., 2016, Mohamad et al., 2017), only a small number of studies have so far focused on the application of interrogators based on Rayleigh back scattering (Monsberger et al., 2016). Using Rayleigh back scattering it is possible to obtain practically continuous high resolution data of strain and temperature inside a pile with a spatial resolution of only a few millimetres, while the spatial resolution is around 0.5 m using Brillouin scattering. The use of distributed fibre optic sensing in

connection to pile testing as compared to spot measurements makes is possible to achieve a previously unseen high degree of detail and increased reliability in the strain measurement and hence a much greater insight into the development and distribution of shaft resistance.

The purpose of this paper is to compare the strain measurements obtained from obtained from Vibrating Wire Strain Gauges (VWSG) and Distributed Fibre Optic Sensors (DFOS) based on Rayleigh back scattering, and to document the use of DFOS for strain measurements in a bored pile.

The paper firstly gives details of the test site conditions and the instrumentation of the pile. The presentation and discussion of results will focus on the correlation between spot and distributed sensors and the distribution of strains in the pile cross section and over the full length of the pile.

2 MATERIALS AND METHODS

2.1 Site conditions

The static pile load test was carried out at a construction site in Viborg, Denmark. The test pile has the same dimensions as the production piles which were designed to support a 6-storey building with parking basement at the lower level.

The boring and CPT profile nearest to the test pile indicate a soil profile consisting of 3.8 m sandy clay fill underlain by a 1.2 m thick layer of buried soft organic sandy clayey top soil on top of sorted late glacial meltwater sand, cf. Figure 1 The meltwater sand continues well below the pile toe and increases in coarseness with depth. Based on the measured cone resistance, q_c from CPT testing, the sand can be classified as medium to very dense. The groundwater table is located at level 19 m ASL (above mean sea level) around 2.7 m above the toe of the test pile.

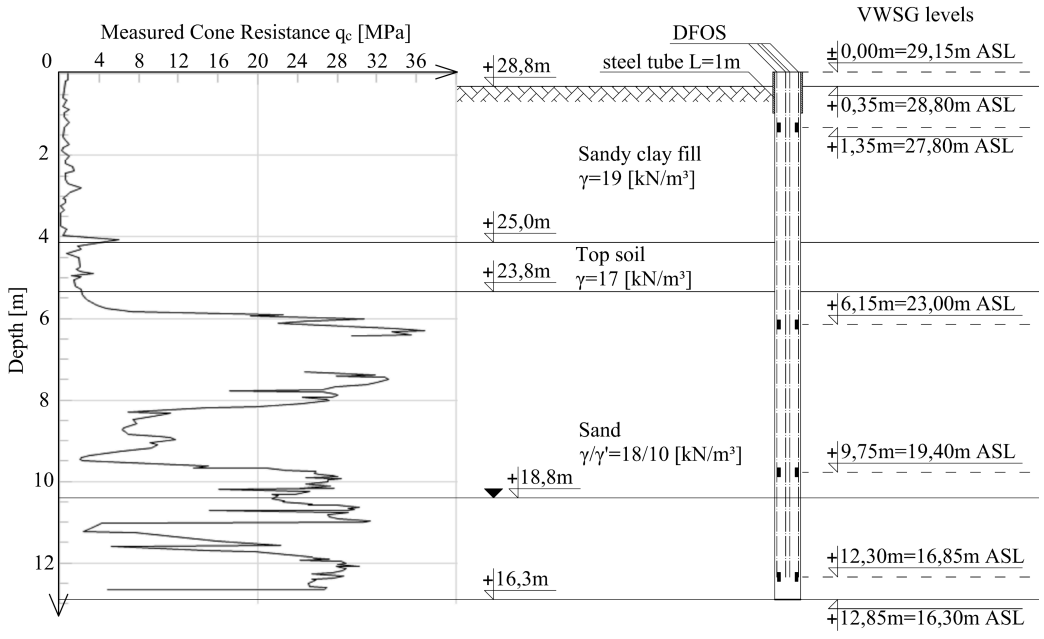

Figure 1. Soil profile and the test pile.

2.2 Test pile

An instrumented, 630 mm diameter, 12,5 m long, cased CFA pile was drilled from a working platform at 28,80 m ASL. The pile head and toe level was 29,15 m ASL and 16,30 m ASL as shown in Figure 1. C35/45 class of concrete was used for the test pile. The 470 mm outer diameter

reinforcing cage consisted of twelve 20 mm diameter main reinforcing bars and 12 mm diameter spiral reinforcement with 150 mm spacing. The bottom 1 m long section of the reinforcing cage was narrowed down to 320 mm diameter using an additional six 20 mm diameter, 1.8 m long main reinforcing bars at the bottom end. The reinforcing cage had additional stiffening rings every 970 mm consisting of 6x60 mm flat bar.

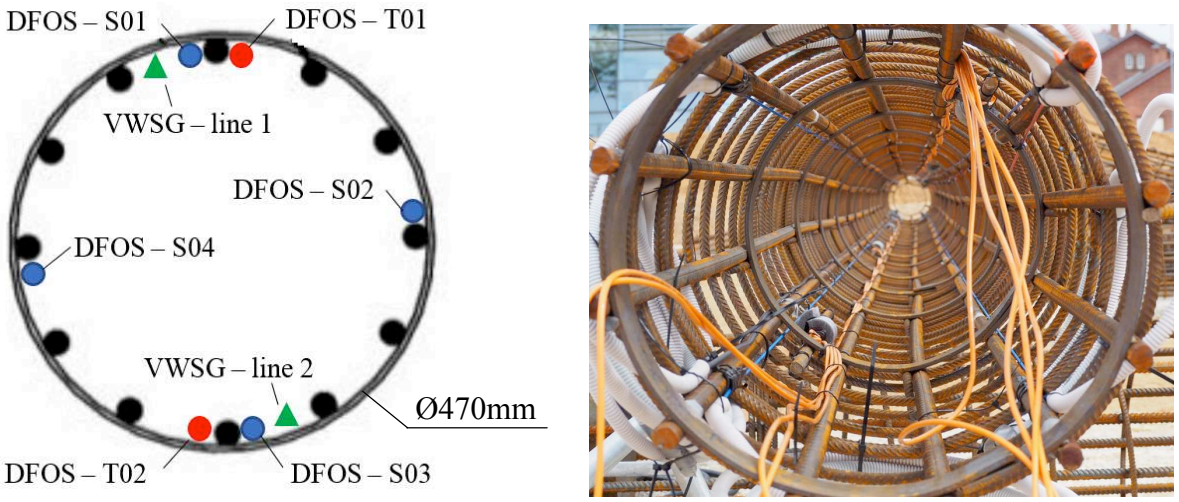

Figure 2. Cross-section of the reinforcement cage showing instrumentation.

Figure 2 shows a photo and illustration of the cross-section of the test pile. As shown in Figure 2 the test pile was instrumented with four lines of strain and two lines of temperature distributed fibre optic sensors (DFOS). A BRUsens V9 strain cable, a BRUsens temperature cable and a standard loose tube gel-filled fibre optical cable (temperature sensor) was used in this case study. The fibre optical sensing cables were fixed to the main reinforcement bars from the pile head to the pile toe. All of strain distributed optical fibre sensing cables were pre-strained to about 700με (cf. Figure 3). Temperature sensing cables were attached on diametrically opposite sides alongside the strain cables as presented in Figure 2. To measure strain and temperature changes, an optical reflectometer based on Rayleigh back scattering was used. The interrogation unit provides data with resolution of about ±1,0με for strain and about ±0,1˚C for temperature measurements. A spatial resolution was set to 2,6 mm. Detailed description of Rayleigh-based distributed fibre-optical sensing techniques was presented by Palmieri and Schenato (Palmieri and Schenato, 2013).

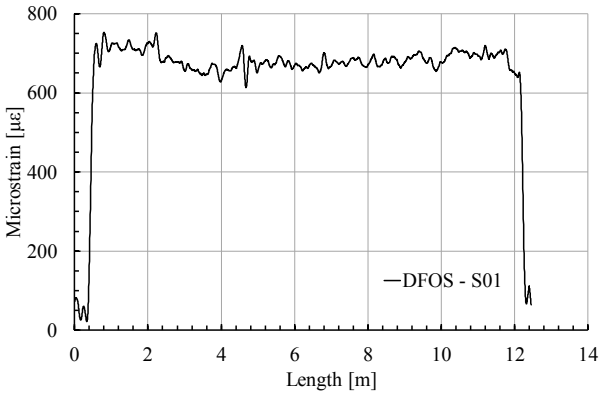

Figure 3. Pre-straining of the fibre optical cable - DFOS-S01.

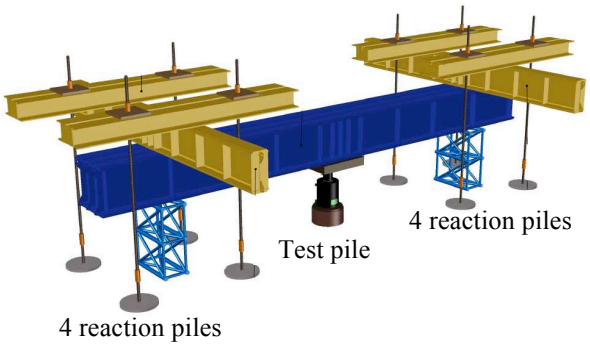

Figure 4. Illustration of the static pile load test setup (Aamann-Svale and Møller, 2017).

In addition to distributed fibre optic sensors, the test pile was instrumented with more traditional 16 mm diameter sister bar vibrating wire strain gauges (VWSG) with a resolution of 0,6με and 50 mm gauge length (shown connected using orange cables in Figure 2). As illustrated in Figure 1 and in the cross-section in Figure 2, two sets of VWSG were installed on diametrically opposite sides at four depths in the pile: 1.35, 6.15, 9.75 and 12.3 m respectively.

2.3 Static pile load test

A static pile load test was performed on the test pile 14 days after installation. Figure 4 illustrates the test setup which makes use of eight reaction piles, four on either side of the test pile and a stiff cross beam. Loads were applied by a computer controlled single hydraulic jack and measured with a load cell. The pile head movement was measured by three displacement transducers attached to a reference frame.

The test was performed as a maintained load (ML) test in which the load is increased in stages to a maximum load with the time/movement curve recorded at each stage of loading and unloading (Tomlinson and Woodward, 2008). As presented in Figure 6, two load cycles were performed. In the first load cycle, the load was applied from initial 0 kN to 1000 kN in 4 increments of each 250 kN and subsequently unloaded in 2 steps of 500 kN. In the second cycle, the load was applied in 9 steps of 250 kN or 500 kN until reaching 4000 kN, and then the pile was unloaded in 2 steps of 2000 kN. The load was maintained for 10 min at each load step before reaching the maximum load in each cycle and maintained for 5 min after each unloading step. After reaching the maximum load in cycle 1 and 2, the load was maintained for 15 min and 30 min respectively.

3 RESULTS

3.1 Static pile load test result

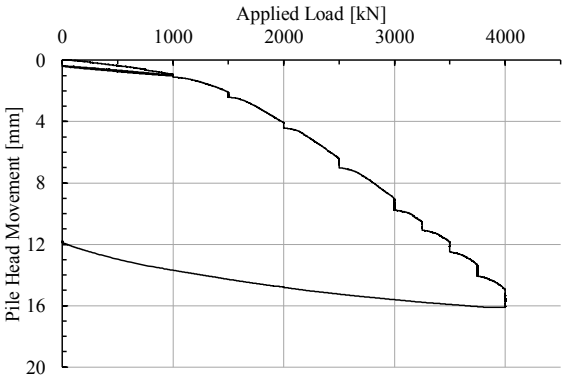

Figure 5. Load-movement curve of the pile head (Aamann-Svale and Møller, 2017).

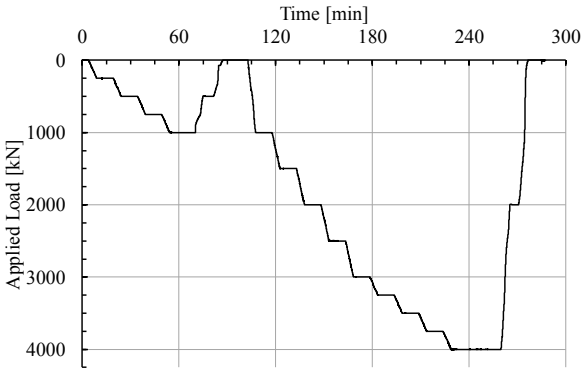

Figure 6. Schedule of the test (Aamann-Svale and Møller, 2017).

Figure 5 shows the load-movement curve at the pile head level. The maximum applied load was 4000kN and the pile head movement at this load was 16 mm, corresponding to around 2.5% of the pile diameter. The load-movement curve does not indicate impeding failure/mobilisation of full capacity in the test. The load-movement response is seen to be very stiff in the first load cycle for loads up to 1000 kN with limited plastic strain generated.

3.2 Measured strain distribution

Figure 7 and Figure 8 present the development in measured strain distribution along the test pile for four selected load steps from 500 kN to 4000 kN obtained from the two sets of sensors that were

placed on diametrically opposite sides; (VWSG-line 1 and DFOS-S01) and (VWSG-line 2 and DFOS-S03) respectively.

Stress free conditions have for simplicity been assumed at the start of the load test. To smoothen the strain profile, a moving average of 40 consecutive reading was used to present data obtained from DFOS (giving a virtual gauge length of roughly 10 cm). The temperature data obtained from VWSG did not indicate any significant change in temperature during the test (±0,1˚C) thus the obtained strain profiles were not thermally compensated.

During the first loading cycle all the DFOS sensors where connected to the interrogation unit through a multi-channel switch. During the second loading cycle only one sensor was directly connected to the interrogator. The more fibre optical connectors are used, the poorer (more scattered) signal can be obtained. To minimize the scatter in the obtained strain measurement in the second load cycle, a new baseline was taken at the end of the first load cycle, and the accumulated strain profile after first load cycle (averaged over 400 readings) was subsequently added to all subsequent readings.

Comparison of strain measurements using DFOS and VWSG

From Figure 7 and Figure 8 a very high correspondence is observed between strain measurements from the vibrating wire strain gauges (VWSG) and distributed fibre optic sensors (DFOS) at the locations of the VWSG. The correspondence of strain measurements is further illustrated in Figure 10 for measurement taken during all load steps.

However, it is also clearly illustrated that distributed fibre optic sensors provide a much more detailed strain profile, which is not possible to obtain from interpolation between the spot measurements using VWSG. For example, it is seen that the soft soil layer located above the sand layer between a depth of 4.1 m and 5.3 m appears to be distinguished from DFOS measurements (constant strain). Furthermore, from Figure 7 the strain profile is shown to yield sharply in the lower part of the test pile (VWSG-line 1 and DFOS-S01) and the exact depth at which it occurs can be clearly seen from the strain profile obtained from DFOS, while the spot measurements only indicate an approximate level.

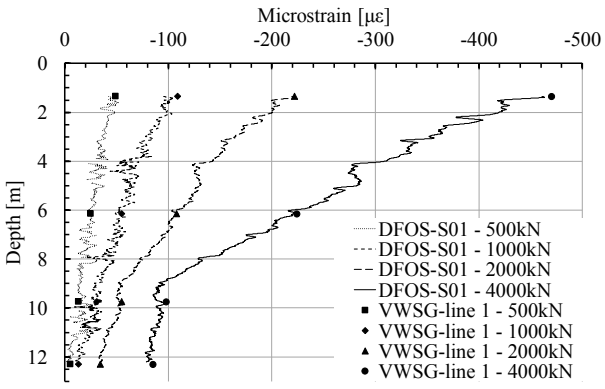

Figure 7. Measured strain distribution of the test pile for selected load steps obtained from VWSG-line 1 and DFOS-S01.

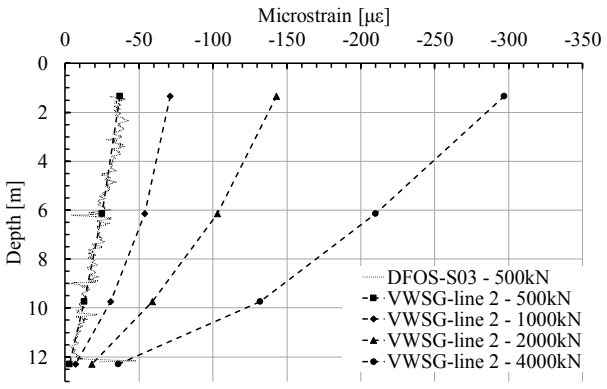

Figure 8. Measured strain distribution of the test pile for selected load steps obtained from VWSG-line 2 and DFOS-S03.

Cross-sectional variation in strain

As shown in Figure 7 and Figure 8, the measured strain profiles may differ significantly depending on the location of a strain sensors set. At the maximum load of 4000 kN VWSG-line 1

and DFOS-S01 sensors recorded around 470 με at the pile head, while VWSG-line 2 sensor showed around 300 με. The percentage difference between those two readings is 44%. The more surprising difference was recorded in the lower part of the test pile. VWSG-line 1 and DFOS-S01 sensors indicate an almost vertical strain profile at the bottom of the test pile with very little change with increasing applied load. In contrast, the strain profile obtained from VWSG-line 2 on the opposite side of the pile is showing significant changes in inclination with increasing loads.

The non-uniformity of strain measurement in different cross-sectional locations and at different levels under the same applied load at the pile head is further illustrated in Figure 9. Although, the strains are non-uniform in the cross section and varies with depth, it is found that if the average strain of opposing strain measurement are compared, then the strain measurements are in very good agreement; e.g. average of VWSG-line 1 and VWSG-line 2 vs. average of DFOS-S02 and DFOS-S04.

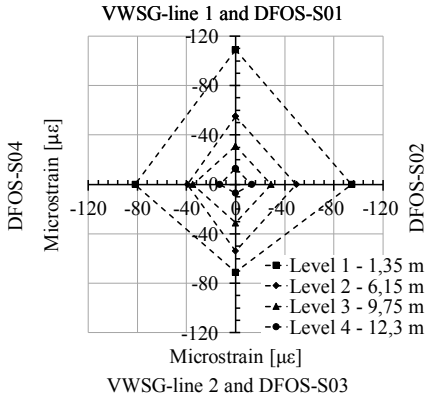

Figure 9. Cross-sectional distribution of strains at four different levels under the pile head load of 1000 kN.

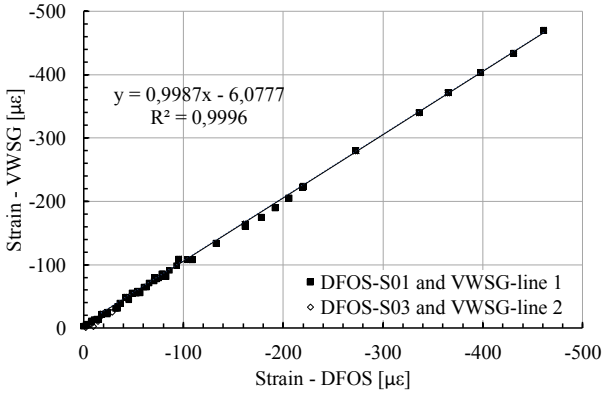

Figure 10. Agreement of strain measurement between VWSG and DFOS sensors located at the same depths

3.3 Back calculated concrete modulus and conversion of strains to axial load

The concrete modulus was back calculated assuming that the load at the first layer of VWSG (1,35m below the pile top) and DFOS was equal to the applied load at the pile head. Furthermore, it is assumed that the concrete modulus is uniform along the pile length. It has not been possible to back calculate the concrete modulus using the tangent method from the lower levels of the pile from the test results, as full shaft resistance may not have been mobilised.

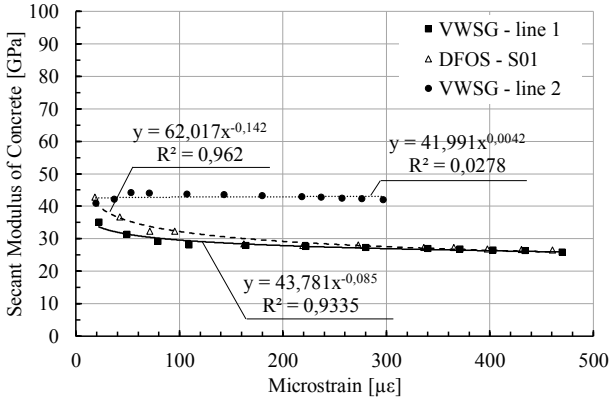

Figure 11. Back-calculated secant modulus of concrete.

In Figure 11the back calculated secant modulus of concrete from VWSG-line 1, VWSG-line 2 and DFOS-S01 strain measurements are plotted against microstrain. It is found that the back calculated secant modulus of concrete from VWSG-line 1 and DFOS-S01 strain measurements are in good agreement, specially at strains above 150 με. The secant modulus of concrete is seen to reduce from around 35-45 GPa at 20 με to around 29 to 30 GPa at 150 με. Above 150 με the modulus is seen only to reduce slightly with increasing strain. The evolution of the secant modulus with strain may with good precision be described by a power function, as shown in Figure 11, as given by the following equations:

$$\text{DFOS-S01: } y=62{,}017\cdot x^{-0{,}142} \quad (1)$$

$$\text{VWSG-line 1: } y=43{,}781\cdot x^{-0{,}085} \quad (2)$$

In contrast, the back calculated secant modulus of concrete from VWSG-line 2 strain measurements give a more or less constant value of secant modulus of 41-44 GPa independent of strain magnitude.

The measured strains were converted to axial load using the equation:

$$F=\varepsilon\cdot(E_C\cdot A_C+E_S\cdot A_S) \quad (3)$$

where: F – axial load, ε – strain reading, E_c – concrete modulus, A_c – cross-sectional area of concrete, E_s – steel modulus, A_s – cross-sectional area of steel reinforcement.

3.4 Mobilised shaft resistance

Figure 12 and Figure 13 shows the average mobilised unit shaft resistance along the test pile in each sublayer derived from the VWSG and DFOS strain data under the maximum applied load of 4000 kN at the pile head.

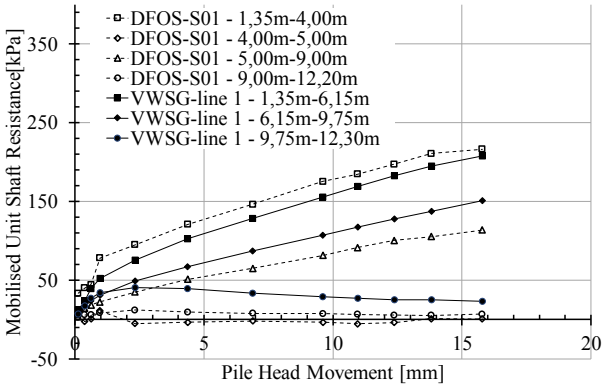

Figure 12. Average mobilised unit shaft resistance in selected sublayers obtained from VWSG-line 1 and DFOS-S01.

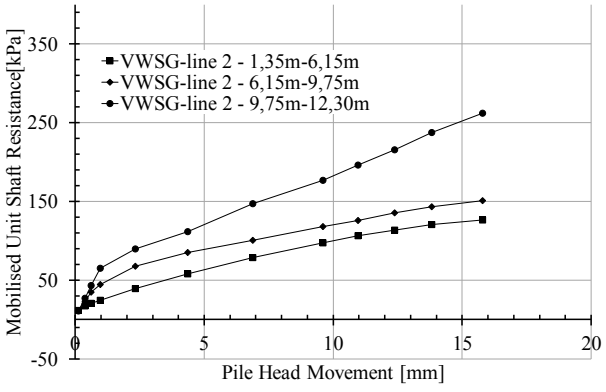

Figure 13. Average mobilised unit shaft resistance in selected sublayers obtained from VWSG-line 2.

From the VWSG data it is only possible to get an average mobilised shaft resistance between the measurement points (three layers), while the DFOS data allows for division into more sensible sublayers based on the characteristics of the strain profile. For the DFOS data a division into four sublayers was chosen.

Based on VWSG-line 1 and DFOS-S01 (Figure 12) it can be seen that strain mobilisation in the lower part is very limited and does not evolve with increasing load. The upper part of the test pile on the other hand show a significant mobilisation of shaft resistance with continues to increase with increasing load. In contrast, based on VWSG-line 2 (Figure 13) the situation is very different especially at the lower end of the pile, where significant shaft resistance is clearly mobilised with increasing load.

4 DISCUSSION AND CONCLUSIONS

In this paper, the results are shown assuming ideal stress-free conditions at the start of the test. This is very likely not the case, as residual forces may arise after pile installation resulting from soil disturbance during pile installation and concrete curing, as discussed by (Mascarucci et al., 2013, Fellenius, 2015). Since the stress conditions at the start of test is very uncertain and due to the measured existence of significant stress non-uniformity in the cross-section of the pile, no attempts have been made in this paper to further interpret the test results and to derive the actual mobilised shaft resistance and end bearing of the test pile.

This study document the use of distributed fibre optic sensors based on Rayleigh scattering for detailed internal strain measurement in a concrete bored pile installed in sand. The strain measurements confirm a high agreement between vibrating wire sister bar gauges strain and distributed fibre optic sensors.

Unlike telltales, the distributed fibre optic sensors can be the primary measurement system because they are installed before pile installation. As opposed to spot sensors, using the distributed fibre optic sensors an engineer does not have to specify the final depths of sensors, because they can measure along its entire length. Owing to this fact, interpolation between sensing points is not needed. The distributed fibre optic sensors based on Rayleigh scattering gives a very detailed strain profile and were able to distinguish internal pile strain variation in different soil layers due to the high spatial resolution of the unit.

The results of this study furthermore highlight the importance of having several sensing points located in the cross section of the pile as strains may be non-uniformely distributed.

ACKNOWLEDGEMENTS

The authors would like to thank cp test a/s, Per Aarsleff A/S, DMT Gründungstechnik GmbH and Innovation Fund Denmark for proving funding for this study and Per Aarsleff A/S for providing data and for installing the instrumented test pile.

REFERENCES

Dunnicliff, J. (1993) *Geotechnical instrumentation for monitoring field performance.* John Wiley & Sons.

Fellenius, B. H. (2002) 'Determining the true distributions of load in instrumented piles', *Deep Foundations 2002: An International Perspective on Theory, Design, Construction, and Performance*, pp. 1455-1470.

Fellenius, B. H. (2015) 'Static tests on instrumented piles affected by residual load', *DFI Journal-The Journal of the Deep Foundations Institute,* 9(1), pp. 11-20.

Kechavarzi, C., Soga, K. B., Battista, N. d., Pelecanos, L., Elshafie, M. Z. E. B., Mair, R. J. and Cambridge Centre for Smart Infrastructure and Construction. (2016) *Distributed fibre optic strain sensing for monitoring civil infrastructure : a practical guide.* London: ICE Publishing, a division of Thomas Telford Ltd.

Mascarucci, Y., Mandolini, A. and Miliziano, S. (2013) 'Effects of residual stresses on shaft friction of bored cast in situ piles in sand', *Journal of Geo-Engineering Sciences,* 1(1), pp. 37-51.

Mohamad, H., Tee, B. P., Chong, M. F. and Ang, K. A. 'Investigation of shaft friction mechanisms of bored piles through distributed optical fibre strain sensing'. *19th International Conference on Soil Mechanics and Geotechnical Engineering*, Seoul.

Monsberger, C., Woschitz, H. and Hayden, M. (2016) 'Deformation measurement of a driven pile using distributed fibre-optic sensing', *Journal of Applied Geodesy,* 10(1), pp. 61-69.

Palmieri, L. and Schenato, L. (2013) 'Distributed optical fiber sensing based on Rayleigh scattering', *The Open Optics Journal,* 7(1).

Siegel, T. C. and McGillivray, A. 'Interpreted residual load in an augered cast-in-place pile'. *Annual DFI Conference*, Kansas City.

Tomlinson, M. and Woodward, J. (2008) *Pile design and construction practice.* Abingdon: Taylor & Francis.

Aamann-Svale, R. and Møller, O. (2017) *Midtbyens Gymnasium, Viborg. Statisk prøvebelasting* (222.437).